Neuro
endocrinology

DOI: 10.1159/000492222
Received: 12/20/2017
Accepted: 7/18/2018
Published(online): 7/19/2018

Establishment and characterization of a novel cell line derived from a small cell neuroendocrine carcinoma of the anal canal
Dizdar L. Drusenheimer J. Werner T. Möhlendick B. Schütte S. Esposito I. Filler T. Knoefel W. Krieg A.

ISSN: 0028-3835 (Print), eISSN: 1423-0194 (Online)
https://www.karger.com/NEN
Neuroendocrinology

Establishment and characterization of a novel cell line derived from a small cell neuroendocrine carcinoma of the anal canal

Levent Dizdar[1], Jasmin Drusenheimer[2], Thomas A. Werner[1], Birte Möhlendick[1], Sina C. Schütte[1], Irene Esposito[2], Timm J. Filler[3], Wolfram T. Knoefel[1], Andreas Krieg[1]

[1]Department of Surgery (A), Heinrich-Heine-University and University Hospital Duesseldorf, Duesseldorf, Germany

[2]Institute of Pathology, Heinrich-Heine-University and University Hospital Duesseldorf, Duesseldorf, Germany

[3]Institute of Anatomy I, Heinrich Heine University Duesseldorf, 40225 Duesseldorf, Germany

Keywords: Gastroenteropancreatic neuroendocrine carcinoma, GEP-NEC, Small cell neuroendocrine carcinoma, Cell culture model

Running title: Establishment of a gastroenteropancreatic small cell neuroendocrine carcinoma cell line

Correspondence to: Andreas Krieg, Department of Surgery (A), Heinrich-Heine-University and University Hospital Duesseldorf, Moorenstr. 5, Bldg. 12.46, 40225 Duesseldorf, Germany; Phone: + 49 211 81 19251; Fax: + 49 211 81 19205; Email: andreas.krieg@med.uni-duesseldorf.de

ABSTRACT

Background: Gastroenteropancreatic neuroendocrine carcinomas (GEP-NECs) are biologically aggressive tumors, associated with a very poor survival. Due to their rarity, our knowledge on GEP-NEC biology is very limited. The aim of this study was to establish a GEP-NEC cell line model that might contribute to a better understanding of this rare malignant disease to further develop novel therapeutic approaches in preclinical studies.

Methods: Small cell neuroendocrine cancer cell line NEC-DUE3 was derived from a lymph node metastasis of a neuroendocrine carcinoma (NEC) located at the anal canal. Morphological characteristics and the expression of neuroendocrine markers were comprehensively investigated. For genetic profiling, NEC-DUE3 cells were analyzed by DNA fingerprinting. Chromosomal aberrations were mapped by array comparative genomic hybridization. NEC-DUE3 cell tumorigenicity was evaluated in vivo and the sensitivity to chemotherapeutic agents was assessed in vitro.

Results: NEC-DUE3 cells were characterized by the expression of molecular markers that are commonly observed in GEP-NECs, were sensitive to treatment with cisplatin and able to form tumors in immunodeficient mice.

Conclusion: We established and characterized the first small cell GEP-NEC cell line that may serve as a valuable tool to create a better understanding of the biology of these rare tumors and to develop novel treatment strategies.

INRODUCTION:

Gastroenteropancreatic neuroendocrine neoplasms (GEP-NENs) consist of a heterogeneous group of tumors characterized by the expression of neuroendocrine marker proteins such as Synaptophysin (SYN) or Chromogranin A (CgA) and can arise in any organ along the digestive tract [1-3]. The WHO classification from 2010 distinguishes GEP-NENs according to their proliferative properties into well (G1: Ki-67 index ≤ 2 %) and moderately (G2: Ki-67 index 3-20 %) differentiated neuroendocrine tumors or poorly differentiated (G3: Ki-67 index > 20 %) neuroendocrine carcinomas (NECs). Furthermore, NECs are categorized according to morphological aspects into large and small cell types. So far, no clear clinicopathological differences between these two morphological subtypes have been shown [4, 5]. However, small cell NECs seem to be more common in organs lined with squamous cell epithelium, like the esophagus and anal canal, whereas large cell NECs are more frequently found in organs with glandular mucosa [5]. Based on their rarity and the limited number of retrospective series and very small non-controlled clinical trials, the optimal therapeutic management of poorly differentiated NECs is unclear [4]. However, in localized disease complete surgical resection offers the only chance for cure [6]. Given the high rate of relapse observed after radical surgery many clinicians recommend adjuvant chemotherapy [7, 8]. Unfortunately, up to 85 % of patients with GEP-NECs have advanced metastatic disease at the time of diagnosis and debulking, cytoreductive surgery or the resection of metastases is not recommended [4, 9, 10]. For these patients palliative chemotherapy with platinum-based drugs combined with etoposide or irinotecan represents the mainstay of treatment [4, 11]. However, response rates of approximately 30 % and a median survival of around one year demonstrate the desperate need for novel treatment approaches [9, 12].

Cell lines derived from human GEP-NEC tissue might be useful tools for the development of novel therapies [13]. Recently, we characterized the two first large cell GEP-NEC cell lines originating from NECs of the gastroesophageal junction and the large intestine [14]. To the

best of our knowledge this is the first report on the establishment and characterization of a cell line derived from a small cell NEC. Cells were characterized by expression profiling of general neuroendocrine marker proteins and tested for tumorigenicity in vivo. Following our previous nomenclature the novel cell line was designated NEC-DUE3.

MATERAILS AND METHODS

Tissue sample processing and cell culture

The establishment of cell lines derived from human tumor tissue was approved by the ethics committee of the Medical Faculty, Heinrich Heine University Duesseldorf (study number: 3457) and written informed consent was obtained from the patient. As described previously, the Medimachine System (BD Biosciences, Heidelberg, Germany) was used to mechanically disassociate fresh tumor tissue samples [14]. The resulting suspension was transferred into 6 well cell culture plates in a final volume of 2 ml RPMI medium (Gibco, Karlsruhe, Germany) supplemented with 10 % heat inactivated FCS (fetal calf serum), penicillin and streptomycin at 37°C in an atmosphere with 5 % CO_2.

Our cell lines NEC-DUE1 and NEC-DUE2 as well as the colon cancer cell line HCT116 served as control in some experiments. Colon cancer cell line HCT116 was obtained from the American Type Culture Collection (ATCC, LGC Standards GmbH, Wesel, Germany) and grown in McCoy´s 5A medium supplemented with 10 % FCS, penicillin and streptomycin. All NEC cell lines were continuously maintained in RPMI medium supplemented with 10 % FCS, penicillin and streptomycin at 37°C and 5 % CO_2.

Immunohistochemistry and immunocytochemistry

Tumor tissue specimens were cut into 2 µm thick sections, mounted on superfrost slides and processed for immunohistochemistry as described previously [14]. For immunocytochemical staining NEC-DUE3 cells were grown on Lab-Tek®Chamber slides and fixed with methanol

and acetone. Specific antibodies as summarized in **Table 1** were used to detect the proteins of interest. Immunostaining was performed using the Vectastatin ABC kit (Vector Lab, Burlingame, CA, USA). In addition, cells and tissue sections were stained with hematoxylin and eosin (H&E) to characterize cellular morphology.

Transmission electron microscopy

Adherent NEC-DUE3 cells were scrapped from the culture dishes, washed in PBS and centrifuged for 10 min. Cell pellets were fixed overnight in 2.5% v/v glutaraldehyde (GA) and 4% w/v paraformaldehyde (PFA) in 0.1 M cacodylate buffer (pH 7.4) at 4 °C. Then, samples were incubated in 1% osmium tetroxide in 0.1 M cacodylate buffer for 2 h. Dehydration was achieved using acetone (30%, 50%, 70%, 90% and 100%) and block contrast was applied (1% phosphotungstic acid/0.5% uranylacetate in 70% acetone). A SPURR embedding kit (Serva, Heidelberg, Germany) was used to embed samples, which were polymerised overnight at 70 °C, before cutting into 80 nm sections using an Ultracut EM UC7 (Leica, Wetzlar, Germany). Ultrathin sections were stained with lead-citrate (according to Reynolds) and 1.5% uranyl-acetate. Images were captured using an H600 TEM (Hitachi, Tokyo, Japan) at 75kV using a Gatan Camera system and were subsequently processed by the Digital Micrograph Software (Gatan, Munich, Germany).

RNA isolation and RT-PCR

Total RNA from cell lines was extracted using the RNeasy Mini Kit (Qiagen, Hilden, Germany). Reverse transcription was performed in a final volume of 20 µl using 0.025 µg oligo-d(T)-primer (Invitrogen/Life Technologies) and Transcriptor Reverse Trancriptase (Roche, Mannheim, Germany). Polymerase chain reaction (PCR) containing 50 ng cDNA was performed as previously described [14]. Primer sequences are summarized in **Table 2**. PCR

products were separated by agarose gel electrophoresis and detected using the Versa Doc system (Bio-RAD, Munich, Germany).

DNA preparation

Genomic DNA (gDNA) from the cell line was prepared using the QIAamp DNA Blood Midi Kit (Qiagen, Hilden, Germany) according to the manufacturer's protocol. DNA from formalin-fixed and paraffin-embedded (FFPE) tissues was isolated utilizing the GeneRead DNA FFPE Kit (Qiagen, Hilden, Germany). Accordingly, areas containing tumor tissue as well as corresponding normal tissue were separately macrodissected with a 20 G needle (Braun, Melsungen, Germany) from a microscopic slide. DNA quality was checked on a 1.5 % agarose gel and DNA quantity was determined using the Infinite 200 PRO NanoQuant spectrophotometer (Tecan Group Ltd., Crailsheim, Germany).

Short Tandem Repeat (STR) Analysis

For DNA fingerprinting analysis, multiplex PCR reactions were performed by amplifying 1 ng of genomic DNA using the PowerPlex® 21 System (Promega, Madison, WI, USA). Amplified products were analyzed on an ABI 3130 Genetic Analyzer capillary sequencer and profiled by the GeneMapper ID V3.2 software (Applied Biosystems, Carlsbad, CA, USA).

Array Comparative Genomic Hybridization (aCGH)

Copy number variations were analyzed using oligonucleotide array-based CGH (Agilent Oligonucleotide Array-Based CGH for Genomic DNA Analysis, Version 7.3; Agilent Technologies, Santa Clara, CA, USA) according to the manufacturer`s instructions and as recently described [14, 15]. Raw microarray image files were processed using the Feature Extraction software (Agilent Technologies, Version 11.5.1.1, Protocol CGH_1200_Jun14) and analyzed with the Genomic Workbench 7.0.4.0 software as previously described [14, 15].

The percentage of aberrant genome (PAG) was determined for each sample. For this analysis, we considered both alteration number and size by translating each alteration into megabase pairs (Mbp), calculated the total size of genomic alterations and divided them by the total genome size (3.15 Gb), respectively.

Cytoxicity assay

For chemotherapeutic drug sensitivity testing, 2×10^4 NEC-DUE3 cells were seeded per well into 96-well plates. After 24 h, cells were treated with increasing concentrations of Cisplatin, Etoposide (both Merck Millipore, Billerica, MA, USA), Oxaliplatin, 5-Fluorouracil (both Sigma-Aldrich, St. Louis, MO, USA) or Octreotide Acetate (Selleckchem, Munich, Germany) for 72 h. All chemicals were dissolved in dimethyl sulfoxide (DMSO). Cell viability was assessed using the CellTiter 96® AQueous Non-Radioactive Cell Proliferation Assay (Promega, Madison, WI, USA). Absorbance of the cell culture medium was measured at a wavelength of 490 nm using the Infinite® 200 microplate reader (Tecan Group Ltd., Crailsheim, Germany). Cell viability is presented as the percentage of the absorbance of treated cells compared to the absorbance of DMSO treated control cells. IC_{50} values were calculated by nonlinear regression (Graph Pad Prism, La Jolla, CA, USA).

Xenograft mouse model

To analyze in vivo tumorigenicity of cell line NEC-DUE3, 1×10^6 cells resuspended in 200 µl of a sterile Matrigel/PBS solution were subcutaneously injected into the flank region of 6 to 8-week-old NOD-Scid IL2rgamma^{null} mice. When tumors became palpable, mice were euthanized. Tumors were carefully removed, fixed in formalin and paraffin embedded for immunohistochemical analysis. All animal experiments were performed in accordance with the German Law for the Protection of Animals and approved by the national supervisory authority in order (Landesamt für Natur, Umwelt und Verbraucherschutz; LANUV NRW: 84-

02.04.2011.A382).

RESULTS

Origin of NEC-DUE3 and histopathological characteristics

A 55-year old Caucasian female presented to our department with a rapidly growing tumor of the anal canal. The histological analysis of a biopsy specimen taken from the primary tumor revealed a small cell GEP-NEC. Whereas accurate preoperative staging excluded distant metastases, computed tomography (CT) scan demonstrated a metastatic involvement of the left inguinal lymph nodes. Accordingly, complete oncological resection was achieved by laparoscopic-assisted abdominoperineal resection of the rectum with terminal sigmoidostomy and left inguinal lymph node dissection with partial resection of the femoral vein **(Figure 1 A and B)**. Both, primary as well as lymph node metastases showed small cell cytology with an immunohistochemically positive staining for neuroendocrine markers synaptophysin and CD56. The marker protein chromogranin A (CgA) was not detected **(Figure 2)**. Approximately 40 % of all tumor cells expressed somatostatin receptor (SSTR) 2A and Ki-67 staining was positive in 90 % of all tumor cells. Whereas pan-cytokeratin (CK) expression and CK8/18 could be observed within the tumor, CK5 or CK20 expression was not detectable. The transcription factors thyroid transcription factor 1 (TTF1), caudal type homeobox 2 (CDX2) and p53 were not expressed, while approximately 20 % of the tumor tissue demonstrated a positive immunohistochemical reaction for retinoblastoma protein (rb1) **(Figure 2)**. Of note, only a very small proportion of cells within the primary demonstrated squamous-cell like morphology with an immunohistochemically positive staining for squamous-cell markers p63 and CK5 (data not shown). According to the latest WHO classification the tumor was staged as a pT2 pN0 (0/7) pM1 (OTH) L0 V1 PN0 R1 G3 (Ki-67 index: 90 %) small cell NEC of the anal canal. The patients' post-operative recovery proceeded without complications except for a mild impairment of wound healing in the left

groin. Adjuvant chemotherapy with 6 cycles of cisplatin and etoposide combined with a radiation therapy to the left inguinal region were recommended by our institutional tumor board.

Cell line properties in vitro and in vivo

Tumor cells isolated from the inguinal metastasis grew as monolayer on conventional cell culture flasks. First, we analyzed the expression profile of general neuroendocrine markers synaptophysin (SYN), chromogranin A (CgA) neuron specific enolase (NSE), cluster of differentiation 56 (CD56), gene product 9.5 (PGP9.5) and SSTR2 by RT-PCR analyses **(Figure 3A)**. Note, GEP-NEC cell lines NEC-DUE1 and 2 served as positive control. In contrast to adenocarcinoma cell line HCT116, mRNA of SYN, NSE, CD56 and PGP 9.5 were expressed in NEC-DUE3 cells. Moreover, SSTR2 transcripts were detectable only in NEC-DUE3 cells.

Next, we investigated the immunocytochemical expression profile of NEC-DUE3 cells. Consistent with the immunohistochemical expression pattern observed within the tumor tissue, staining for pan-CK, SYN, SSTR2A and rb1 was positive in NEC-DUE3 cells, chromogranin A (CgA), p53 and squamous-cell markers p63 and CK5 were undetectable (**Figure 3B**). As the clinical grading of GEP-NENs is assessed by immunohistochemical staining for the nuclear proliferation factor Ki-67, we also analyzed Ki-67 expression in NEC-DUE3 cells. Similar to the patient's original tumor almost all NEC-DUE3 cells were positive for this proliferation marker (Ki-67 index = 90 %) **(Figure 3B)**.

The presence of electron dense neurosecretory granules represents a typical morphological feature of neuroendocrine cells [16]. Hence, we performed transmission electron microscopy of our novel cell line NEC-DUE3. Surprisingly, we could only rarely detect structures compatible with neurosecretory granules in NEC-DUE3 cells **(Figure 4)**.

To date, NEC-DUE3 cells proliferate for more than 30 passages and recovery of

cryopreserved cells presented no problems. Importantly, we did not detect any changes in morphology or growth pattern with increasing passages.

Cytogenetic characterization

In order to confirm the authenticity of cell line NEC-DUE3, we performed STR-analysis comparing DNA isolated from primary and metastatic tumor tissue specimens as well as NEC-DUE3 cells. As expected, STR profiles of NEC-DUE3 cells matched to specific regions on the DNA of both primary and metastatic tumor (**Table 3**). Furthermore, we analyzed cytogenetic changes in the primary tumor, the inguinal lymph node metastasis and NEC-DUE3 cells by aCGH analyses (**Figure 5**). These analyses revealed obvious differences between the primary tumor (PT) and its inguinal lymph node metastasis (LNMET). In contrast, genetic alterations in NEC-DUE3 cells were similar to those of the LNMET they were isolated from. Thus, aCGH results reconfirmed the origin of NEC-DUE3 cells from the inguinal lymph node metastasis. Interestingly, the percentage of genomic alterations was three to four times higher in NEC-DUE3 cells (45.49 %) and the lymph node metastasis (34.25 %) when compared to the primary tumor (10.47 %). The most common chromosomal gains were located on chromosomes 1, 6, 8, 9, 17 and 20, whereas chromosomes 2, 10 and 15 were affected by chromosomal losses.

Response to chemotherapeutic agents

Combinational chemotherapy including cisplatin and etoposide represents the first line therapy for advanced G3 GEP-NECs [4]. Although no standard salvage therapy for patients with tumor progression during first line therapy exists, small series documented response rates of up to 40 % using oxaliplatin and 5-fluoruracil (5-FU) based regimens [4]. On the basis of these findings, we incubated NEC-DUE3 cells with increasing concentrations of cisplatin, etoposide, oxaliplatin and 5-FU. Since NEC-DUE3 cells expressed SSTR2A we

also investigated their response to a somatostatin receptor-targeted therapy.

NEC-DUE3 cells showed a drug response within the screening concentrations of cisplatin, etoposide, oxaliplatin and 5-FU. However, only for cisplatin the IC_{50} value was lower than the maximum chemotherapeutic concentration used in our in vitro experiments (**Figure 6A**). In contrast, octreotide did not affect cell viability of NEC-DUE3 cells.

Tumorigenicity in vivo

To assess the tumorigenicity of NEC-DUE3 cells we subcutaneously injected 1×10^6 cells into the flank region of 6 to 8-week-old NOD/SCID immunodeficient mice. Three weeks after injection tumor nodules became palpable and mice were sacrificed **(Figure 6B)**. As expected, the histopathological and immunohistochemical examination of tumor tissue specimens from NEC-DUE3 xenografts revealed the typical morphology of a highly proliferative and synaptophysin-positive small cell NEC (**Figure 6C**).

DISCUSSION

According to the current WHO classification all GEP neuroendocrine tumors with a Ki-67 index > 20 % are categorized as poorly differentiated GEP-NEC. GEP-NECs are very rare neoplasms accounting for less than 1 % of all gastrointestinal malignancies and approximately 10 % of all GEP-NENs [17]. Typical locations are the esophagus, pancreas, large bowel and very rarely the ileum or the anal canal [7, 9, 18]. Already at the time of diagnosis 65 % of patients with GEP-NECs have distant metastasis, which are most frequently located in the liver (70 %), followed by lung (15 %) and bone (15 %) [4, 9]. To date, therapy approaches for GEP-NECs are largely adopted from treatment strategies of small cell lung cancer (SCLC) [19-22]. Median survival rates for GEP-NEC reported in recent studies range from 4 to 16 months [7, 9, 10, 17, 21-24]. In this context it becomes evident that there is an urgent need for novel therapeutic strategies specifically developed for GEP-NEC. An important prerequisite

for the realization of this objective is a better understanding of GEP-NEC biology and the possibility to establish novel treatment strategies in preclinical models. For this purpose GEP-NEC cell lines might provide helpful tools.

Recently, we characterized two large cell GEP-NEC cell lines derived from a gastroesophageal and a colorectal NEC that have already successfully been used in a preclinical model [14, 25]. In this study, we now report on the establishment and characterization of the first small cell GEP-NEC cell line. The primary tumor, which was located in the anal canal, exhibited a typical neuroendocrine morphology and marker profile in the greater part of the tumor. Only a very small fraction of the primary tumor cells showed a squamous-cell differentiation. The large inguinal lymph node metastasis, which infiltrated the whole lymphatic compartment of the left groin, exclusively demonstrated immunohistochemical patterns of a small cell NEC.

Importantly, NEC-DUE3 cell line originating from the inguinal metastasis showed only a neuroendocrine morphology and marker profile. NEC-DUE3 cells expressed neuroendocrine markers SYN, CD56, NSE and PGP 9.5 but were negative for CgA. Note, SYN and CgA are the most specific neuroendocrine markers for GEP-NEN [26]. However, whereas SYN is always expressed in GEP-NECs, CgA immunoreactivity in GEP-NECs is rather rarely detectable. In this context, Li et al. determined neuroendocrine marker expression in 42 small cell GEP-NECs. They demonstrated that SYN and NSE were found in 100% and CD56 in 90.5% of small cell GEP-NECs, whereas only 61.9% stained positive for CgA [27]. In addition, Benten et al., who thoroughly characterized three pancreatic NEN cell lines, observed low SYN and particularly CgA expression levels in highly proliferative BON and QGP-1 cells, whereas well-differentiated NT-3 cells were characterized by high SYN and CgA expression [28]. The authors concluded, that low neuroendocrine marker expression in GEP-NEN cell lines is related to a more malignant phenotype. Taken together the profile of neuroendocrine markers expressed in NEC-DUE3 cells clearly demonstrates the

neuroendocrine origin of this novel cell line. In addition, we could verify a high proliferative activity of NEC-DUE3 cells by Ki-67 staining, corresponding to the highly proliferative G3 NEC they were isolated from.

In order to confirm the neuroendocrine nature of the novel cell line we finally performed transmission electron microscopy of NEC-DUE3 cells. Surprisingly and in contrast to our previously established large cell GEP-NEC cell lines NEC-DUE1 and NEC-DUE2 we could only rarely detect structures compatible with neurosecretory granules in NEC-DUE3 cells. However, in this context it should be mentioned that published studies analyzing the ultrastructure of small cell NECs of the lung or prostate also detected secretory granules only infrequently [29-31]. For example Farhat et al. identified significantly less secretory granules in small cell NECs of the lung when compared to large cell NECs [29]. Furthermore, Vollmer et al. noted that dense core granules were absent in 11.5 % and only occasionally found in 42 % of small cell NECs of the lung [31]. In view of these publications as well as the electron microscopic analysis of our cell line, neurosecretory granules seem to be rare or even absent in many small cell NECs.

In order to reliably exclude a contamination of our neuroendocrine cell line with squamous-cell carcinoma cells, we performed a immunocytochemical staining for squamous-cell markers p63 and CK5, which both were expressed in the squamous-cell carcinoma component of the primary tumor. Importantly, our data clearly demonstrated that both markers were not detectable in NEC-DUE3 cells. In addition, aCGH analysis revealed similar chromosomal alterations in NEC-DUE3 cells and the original inguinal lymph node metastasis, further reconfirming the origin of NEC-DUE3 cells from the inguinal metastasis. Increased genomic alterations have been associated with GEP-NEN progression [32]. In line with these findings the percentage of chromosomal alterations was three to four times higher in the inguinal metastasis and NEC-DUE3 cells when compared to the primary tumor. In addition, we detected a gain of chromosome 20q in the cell line, the primary tumor and the lymph node

metastasis, which has been described as a frequent alteration in GEP-NENs [32]. However, we did not observe a partial or complete loss of chromosome 18 or a gain of chromosome 7p, which have also been reported to be common alterations in GEP-NENs [32-34].

To assess the sensitivity of our small cell NEC cell line to chemotherapy, we incubated NEC-DUE3 cells with increasing concentrations of common chemotherapeutic drugs. Notably, NEC-DUE3 cells demonstrated a significant reduction in cell viability when incubated with cisplatin but showed only little response to a treatment with etoposide, oxaliplatin and 5-FU in vitro. First-line chemotherapy for GEP-NECs consists of a combinational therapy including cisplatin and etoposide [4, 11, 35]. Recent studies reported low response rates of only 17 to 37.5 % to this chemotherapeutic regimen [22, 36-38]. A widely discussed question concerning the use of chemotherapeutics for GEP-NEC treatment is whether a Ki-67 index cut-off point for response to chemotherapy exists. Interestingly, patients with highly proliferative GEP-NECs (Ki-67 index > 55 %) were characterized by a significantly worse survival but responded better to platinum based chemotherapy when compared to GEP-NECs with a Ki-67 index < 55 % [9, 39, 40]. Accordingly, the high proliferative activity of NEC-DUE3 cells (Ki-67 index of 90 %) might explain the good response to cisplatin.

Even though NEC-DUE3 cells widely expressed SSTR2A they did not respond to somatostatin treatment at all. Similar results were observed in previously published studies analyzing the effects of octreotide in BON, QCP-1 and LCC-18 cell lines [28, 41]. In line with these findings, the current European guidelines for the treatment of GEP-NECs do not support the use of somatostatin analogs even in patients with somatostatin receptor positive tumors [4].

Finally, we confirmed the in vivo tumorigenicity of NEC-DUE3 cells using an in vivo mouse model in which tumor cells retained their morphological characteristics and neuroendocrine marker profile.

In summary, NEC-DUE3 is the third GEP-NEC cell line established in our laboratory and to our knowledge the first small cell GEP-NEC cell line reported so far. NEC-DUE3 cells exhibited a highly proliferative, aggressive and chemoresistant phenotype and might serve as a helpful tool to analyze neuroendocrine cancer biology and to develop novel strategies in the treatment of poorly differentiated GEP-NECs.

ACKNOWLEDGEMENTS

The study was supported, in part, by a grant from the Forschungskommission of the Medical Faculty, University Duesseldorf (39/2014 to AK and TAW)

REFERENCES

1. Buffa R, Rindi G, Sessa F, Gini A, Capella C, Jahn R, Navone F, De Camilli P, Solcia E: Synaptophysin immunoreactivity and small clear vesicles in neuroendocrine cells and related tumours. Mol Cell Probes 1987;1:367-81.
2. Wiedenmann B, John M, Ahnert-Hilger G, Riecken EO: Molecular and cell biological aspects of neuroendocrine tumors of the gastroenteropancreatic system. J Mol Med (Berl) 1998;76:637-47.
3. Rindi G, Buffa R, Sessa F, Tortora O, Solcia E: Chromogranin A, B and C immunoreactivities of mammalian endocrine cells. Distribution, distinction from costored hormones/prohormones and relationship with the argyrophil component of secretory granules. Histochemistry 1986;85:19-28.
4. Garcia-Carbonero R, Sorbye H, Baudin E, Raymond E, Wiedenmann B, Niederle B, Sedlackova E, Toumpanakis C, Anlauf M, Cwikla JB, Caplin M, O'Toole D, Perren A, Vienna Consensus Conference p: ENETS Consensus Guidelines for High-Grade Gastroenteropancreatic Neuroendocrine Tumors and Neuroendocrine Carcinomas. Neuroendocrinology 2016;103:186-94.
5. Shia J, Tang LH, Weiser MR, Brenner B, Adsay NV, Stelow EB, Saltz LB, Qin J, Landmann R, Leonard GD, Dhall D, Temple L, Guillem JG, Paty PB, Kelsen D, Wong WD, Klimstra DS: Is nonsmall cell type high-grade neuroendocrine carcinoma of the tubular gastrointestinal tract a distinct disease entity? Am J Surg Pathol 2008;32:719-31.
6. Sauven P, Ridge JA, Quan SH, Sigurdson ER: Anorectal carcinoid tumors. Is aggressive surgery warranted? Ann Surg 1990;211:67-71.
7. Brenner B, Shah MA, Gonen M, Klimstra DS, Shia J, Kelsen DP: Small-cell carcinoma of the gastrointestinal tract: a retrospective study of 64 cases. Br J Cancer 2004;90:1720-6.
8. Casas F, Ferrer F, Farrus B, Casals J, Biete A: Primary small cell carcinoma of the esophagus: a review of the literature with emphasis on therapy and prognosis. Cancer 1997;80:1366-72.
9. Sorbye H, Welin S, Langer SW, Vestermark LW, Holt N, Osterlund P, Dueland S, Hofsli E, Guren MG, Ohrling K, Birkemeyer E, Thiis-Evensen E, Biagini M, Gronbaek H, Soveri LM, Olsen IH, Federspiel B, Assmus J, Janson ET, Knigge U: Predictive and prognostic factors for treatment and survival in 305 patients with advanced gastrointestinal neuroendocrine carcinoma (WHO G3): the NORDIC NEC study. Ann Oncol 2013;24:152-60.
10. Garcia-Carbonero R, Capdevila J, Crespo-Herrero G, Diaz-Perez JA, Martinez Del Prado MP, Alonso Orduna V, Sevilla-Garcia I, Villabona-Artero C, Beguiristain-Gomez A, Llanos-Munoz M, Marazuela M, Alvarez-Escola C, Castellano D, Vilar E, Jimenez-Fonseca P, Teule A, Sastre-Valera J, Benavent-Vinuelas M, Monleon A, Salazar R: Incidence, patterns of care and prognostic factors for outcome of gastroenteropancreatic neuroendocrine tumors (GEP-NETs): results from the National Cancer Registry of Spain (RGETNE). Ann Oncol 2010;21:1794-803.
11. Pavel M, Baudin E, Couvelard A, Krenning E, Oberg K, Steinmuller T, Anlauf M, Wiedenmann B, Salazar R, Barcelona Consensus Conference p: ENETS Consensus Guidelines for the management of patients with liver and other distant metastases from neuroendocrine neoplasms of foregut, midgut, hindgut, and unknown primary. Neuroendocrinology 2012;95:157-76.

12. Strosberg J, Nasir A, Coppola D, Wick M, Kvols L: Correlation between grade and prognosis in metastatic gastroenteropancreatic neuroendocrine tumors. Hum Pathol 2009;40:1262-8.
13. Rockwell S: In vivo-in vitro tumour cell lines: characteristics and limitations as models for human cancer. Br J Cancer Suppl 1980;4:118-22.
14. Krieg A, Mersch S, Boeck I, Dizdar L, Weihe E, Hilal Z, Krausch M, Mohlendick B, Topp SA, Piekorz RP, Huckenbeck W, Stoecklein NH, Anlauf M, Knoefel WT: New model for gastroenteropancreatic large-cell neuroendocrine carcinoma: establishment of two clinically relevant cell lines. PLoS One 2014;9:e88713.
15. Mohlendick B, Stoecklein NH: Analysis of Copy-Number Alterations in Single Cells Using Microarray-Based Comparative Genomic Hybridization (aCGH). Curr Protoc Cell Biol 2014;65:22 19 1-23.
16. Pearse AG: The cytochemistry and ultrastructure of polypeptide hormone-producing cells of the APUD series and the embryologic, physiologic and pathologic implications of the concept. J Histochem Cytochem 1969;17:303-13.
17. Pape UF, Bohmig M, Berndt U, Tiling N, Wiedenmann B, Plockinger U: Survival and clinical outcome of patients with neuroendocrine tumors of the gastroenteropancreatic tract in a german referral center. Ann N Y Acad Sci 2004;1014:222-33.
18. Sorbye H, Strosberg J, Baudin E, Klimstra DS, Yao JC: Gastroenteropancreatic high-grade neuroendocrine carcinoma. Cancer 2014;120:2814-23.
19. Brennan SM, Gregory DL, Stillie A, Herschtal A, Mac Manus M, Ball DL: Should extrapulmonary small cell cancer be managed like small cell lung cancer? Cancer 2010;116:888-95.
20. Walenkamp AM, Sonke GS, Sleijfer DT: Clinical and therapeutic aspects of extrapulmonary small cell carcinoma. Cancer Treat Rev 2009;35:228-36.
21. Cicin I, Karagol H, Uzunoglu S, Uygun K, Usta U, Kocak Z, Caloglu M, Saynak M, Tokatli F, Uzal C: Extrapulmonary small-cell carcinoma compared with small-cell lung carcinoma: a retrospective single-center study. Cancer 2007;110:1068-76.
22. Terashima T, Morizane C, Hiraoka N, Tsuda H, Tamura T, Shimada Y, Kaneko S, Kushima R, Ueno H, Kondo S, Ikeda M, Okusaka T: Comparison of chemotherapeutic treatment outcomes of advanced extrapulmonary neuroendocrine carcinomas and advanced small-cell lung carcinoma. Neuroendocrinology 2012;96:324-32.
23. Formica V, Wotherspoon A, Cunningham D, Norman AR, Sirohi B, Oates J, Chong G: The prognostic role of WHO classification, urinary 5-hydroxyindoleacetic acid and liver function tests in metastatic neuroendocrine carcinomas of the gastroenteropancreatic tract. Br J Cancer 2007;96:1178-82.
24. Ilett EE, Langer SW, Olsen IH, Federspiel B, Kjaer A, Knigge U: Neuroendocrine Carcinomas of the Gastroenteropancreatic System: A Comprehensive Review. Diagnostics (Basel) 2015;5:119-76.
25. Dizdar L, Oesterwind KA, Riemer JC, Werner TA, Mersch S, Mohlendick B, Schutte SC, Verde PE, Raba K, Topp SA, Stoecklein NH, Esposito I, Knoefel WT, Krieg A: Preclinical assesement of survivin and XIAP as prognostic biomarkers and therapeutic targets in gastroenteropancreatic neuroendocrine neoplasia. Oncotarget 2017;8:8369-82.
26. Rindi G, Wiedenmann B: Neuroendocrine neoplasms of the gut and pancreas: new insights. Nat Rev Endocrinol 2011;8:54-64.
27. Li AF, Li AC, Hsu CY, Li WY, Hsu HS, Chen JY: Small cell carcinomas in gastrointestinal tract: immunohistochemical and clinicopathological features. J Clin Pathol 2010;63:620-5.
28. Benten D, Behrang Y, Unrau L, Weissmann V, Wolters-Eisfeld G, Burdak-Rothkamm S, Stahl FR, Anlauf M, Grabowski P, Mobs M, Dieckhoff J, Sipos B, Fahl M, Eggers

C, Perez D, Bockhorn M, Izbicki JR, Lohse AW, Schrader J: Establishment of the First Well-differentiated Human Pancreatic Neuroendocrine Tumor Model. Mol Cancer Res 2018;16:496-507.
29. Farhat CA, Parra ER, Rogers AV, Elian SN, Sheppard MN, Capelozzi VL: Using electron microscopy and multivariate cluster analysis to determine diagnosis and prognosis in cases of neuroendocrine lung carcinoma. J Bras Pneumol 2008;34:804-11.
30. Ro JY, Tetu B, Ayala AG, Ordonez NG: Small cell carcinoma of the prostate. II. Immunohistochemical and electron microscopic studies of 18 cases. Cancer 1987;59:977-82.
31. Vollmer RT, Shelburne JD, Iglehart JD: Intercellular junctions and tumor stage in small cell carcinoma of the lung. Hum Pathol 1987;18:22-7.
32. Zhao J, de Krijger RR, Meier D, Speel EJ, Saremaslani P, Muletta-Feurer S, Matter C, Roth J, Heitz PU, Komminoth P: Genomic alterations in well-differentiated gastrointestinal and bronchial neuroendocrine tumors (carcinoids): marked differences indicating diversity in molecular pathogenesis. Am J Pathol 2000;157:1431-8.
33. Lollgen RM, Hessman O, Szabo E, Westin G, Akerstrom G: Chromosome 18 deletions are common events in classical midgut carcinoid tumors. Int J Cancer 2001;92:812-5.
34. Terris B, Meddeb M, Marchio A, Danglot G, Flejou JF, Belghiti J, Ruszniewski P, Bernheim A: Comparative genomic hybridization analysis of sporadic neuroendocrine tumors of the digestive system. Genes Chromosomes Cancer 1998;22:50-6.
35. Janson ET, Sorbye H, Welin S, Federspiel B, Gronbaek H, Hellman P, Ladekarl M, Langer SW, Mortensen J, Schalin-Jantti C, Sundin A, Sundlov A, Thiis-Evensen E, Knigge U: Nordic guidelines 2014 for diagnosis and treatment of gastroenteropancreatic neuroendocrine neoplasms. Acta Oncol 2014;53:1284-97.
36. Velayoudom-Cephise FL, Duvillard P, Foucan L, Hadoux J, Chougnet CN, Leboulleux S, Malka D, Guigay J, Goere D, Debaere T, Caramella C, Schlumberger M, Planchard D, Elias D, Ducreux M, Scoazec JY, Baudin E: Are G3 ENETS neuroendocrine neoplasms heterogeneous? Endocr Relat Cancer 2013;20:649-57.
37. Hentic O, Couvelard A, Rebours V, Zappa M, Dokmak S, Hammel P, Maire F, O'Toole D, Levy P, Sauvanet A, Ruszniewski P: Ki-67 index, tumor differentiation, and extent of liver involvement are independent prognostic factors in patients with liver metastases of digestive endocrine carcinomas. Endocr Relat Cancer 2011;18:51-9.
38. Deutschbein T, Unger N, Yuece A, Eberhardt W, Gauler T, Lahner H, Mann K, Petersenn S: Chemotherapy in patients with progressive, undifferentiated neuroendocrine tumors: a single-center experience. Horm Metab Res 2011;43:838-43.
39. Olsen IH, Sorensen JB, Federspiel B, Kjaer A, Hansen CP, Knigge U, Langer SW: Temozolomide as second or third line treatment of patients with neuroendocrine carcinomas. ScientificWorldJournal 2012;2012:170496.
40. Welin S, Sorbye H, Sebjornsen S, Knappskog S, Busch C, Oberg K: Clinical effect of temozolomide-based chemotherapy in poorly differentiated endocrine carcinoma after progression on first-line chemotherapy. Cancer 2011;117:4617-22.
41. Exner S, Prasad V, Wiedenmann B, Grotzinger C: Octreotide Does Not Inhibit Proliferation in Five Neuroendocrine Tumor Cell Lines. Front Endocrinol (Lausanne) 2018;9:146.

TABLES AND FIGURES

Table 1: Antibodies used for immunohistochemistry and immunocytochemistry

Table 2: Primers used for RT-PCR

Table 3: STR analysis of the primary tumor (PT), the lymph node metastasis (LNMET) and NEC-DUE3 cell line

Figure 1: Intraoperative findings demonstrating the conglomeration of metastatic inguinal lymph nodes. (A) The inguinal lymph node metastases infiltrating the femoral vein. **(B)** Inguinal metastasis after longitudinal incision (white arrow marks the femoral vein; black arrow highlights the inguinal lymph node metastasis).

Figure 2: Morphological and immunohistochemical characterization of the primary tumor. Staining with hematoxylin-eosin (HE) demonstrates small cell neuroendocrine cancer morphology. Synaptophysin (SYN), chromogranin A (CgA), cluster of differentiation 56 (CD56), somatostatin receptor 2A (SSTR2A), cytokeratins (CK), thyroid transcription factor 1 (TTF1), caudal type homeobox 2 (CDX2), p53 and retinoblastoma protein (rb1) were immunohistochemically evaluated as indicated. Mitotic activity was analyzed by Ki-67 staining. Images were captured at 400 × magnification and scale bar indicates 25 µm.

Figure 3: NEC-DUE3 cell line expresses neuroendocrine markers. (A) RNA from NEC-DUE3 cells was isolated and analyzed by RT-PCR for the expression of neuroendocrine markers Synaptophysin (SYN), chromogranin A (CgA), neuron specific enolase (NSE), cluster of differentiation 56 (CD56), gene product 9.5 (PGP9.5) and somatostatinreceptor 2A

(SSTR2A). The neuroendocrine cancer cell lines NEC-DUE1 and NEC-DUE2 as well as the colon cancer cell line HCT116 served as controls. **(B)** NEC-DUE3 cells were grown on chamber slides and stained with hematoxylin-eosin (HE). The expression of cytokeratins (CK), synaptophysin (SYN), chromogranin A (CgA), Ki-67, somatostatin receptor 2A (SSTR2A), p63, cytokeratin 5 (CK5), p53 and retinoblastoma protein (rb1) was analyzed by immunohistochemistry. Images were captured at 400 × magnification and scale bar indicates 25 µm.

Figure 4: Transmission electron microscopy of NEC-DUE3 cells. (A) Electron microscopy revealed only rare structures compatible with neurosecretory granules in NEC-DUE3 cells (black square marks the section of Figure 4B). **(B)** Magnified section demonstrating one example of an electron-dense particle compatible with a neurosecretory granule localized in the cytoplasm of a NEC-DUE3 cell (black arrow highlights the potential neurosecretory granule).

Figure 5: Cytogenetic changes in the primary tumor (PT), the lymph node metastasis (LNMET) and NEC-DUE3 cell line. DNA was isolated from the cell line, the primary tumor (PT) and the inguinal lymph node metastasis (LNMET). Genetic alterations were analyzed by aCGH analysis. Amplitudes over the midline reflect chromosomal gains, amplitudes under the midline losses.

Figure 6: In vitro sensitivity to chemotherapeutic drugs and in vivo tumorigenicity of NEC-DUE3 cells. (A) Sensitivity of NEC-DUE3 cells to conventional chemotherapeutics and somatostatin. Cell viability was measured using the MTS assay as described in materials and methods. Values represent the mean percentage of the absorbance of treated cells compared to the absorbance of DMSO treated control cells ± standard error of mean (SEM) of triplicates.

(B) Xenografts were removed from immunocompromized mice 21 days after subcutaneous injection of NEC-DUE3 cells. **(C)** FFPE sections from tumor nodules were stained with hemtoxylin-eosin (HE) and analyzed for the expression of synaptophysin (SYN) and Ki-67. Images were captured at 400 × magnification and scale bar indicates 25 μm.

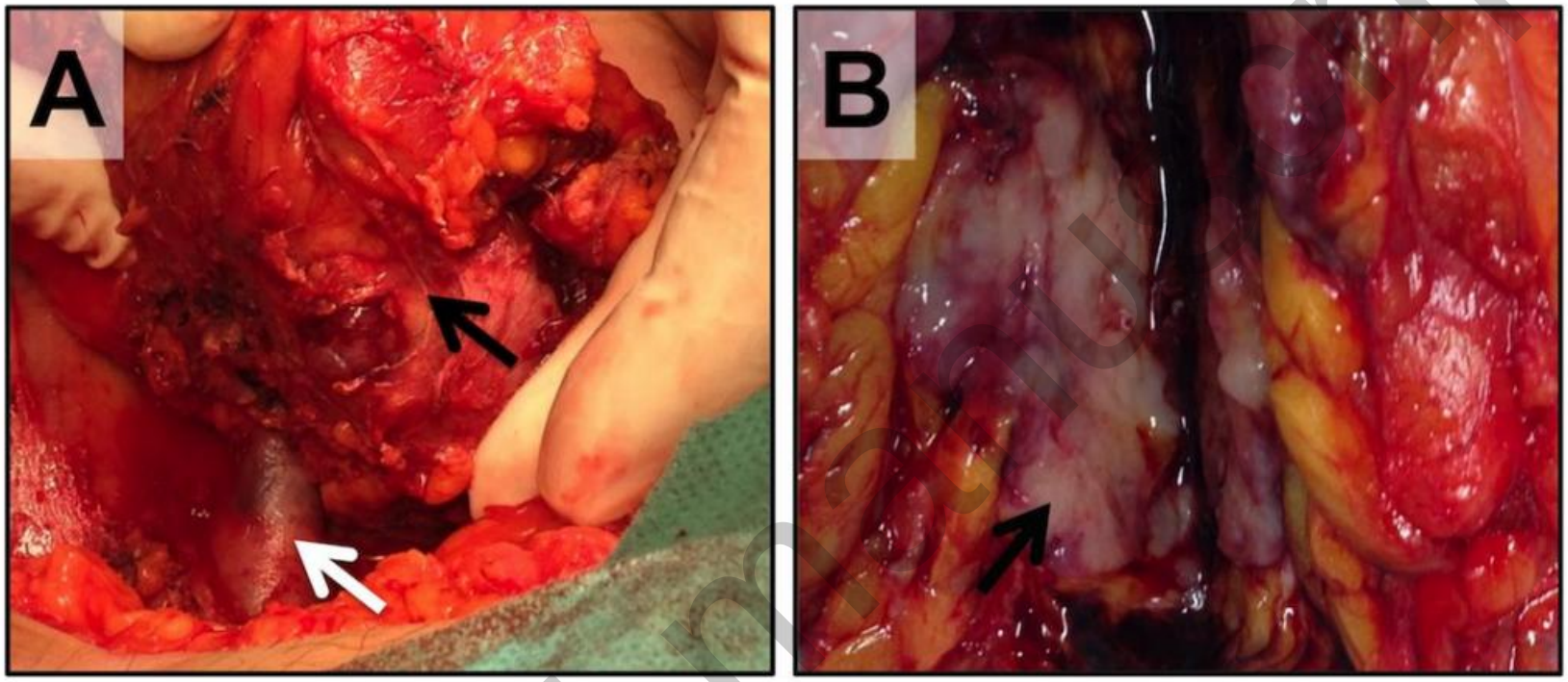

Figure 1.

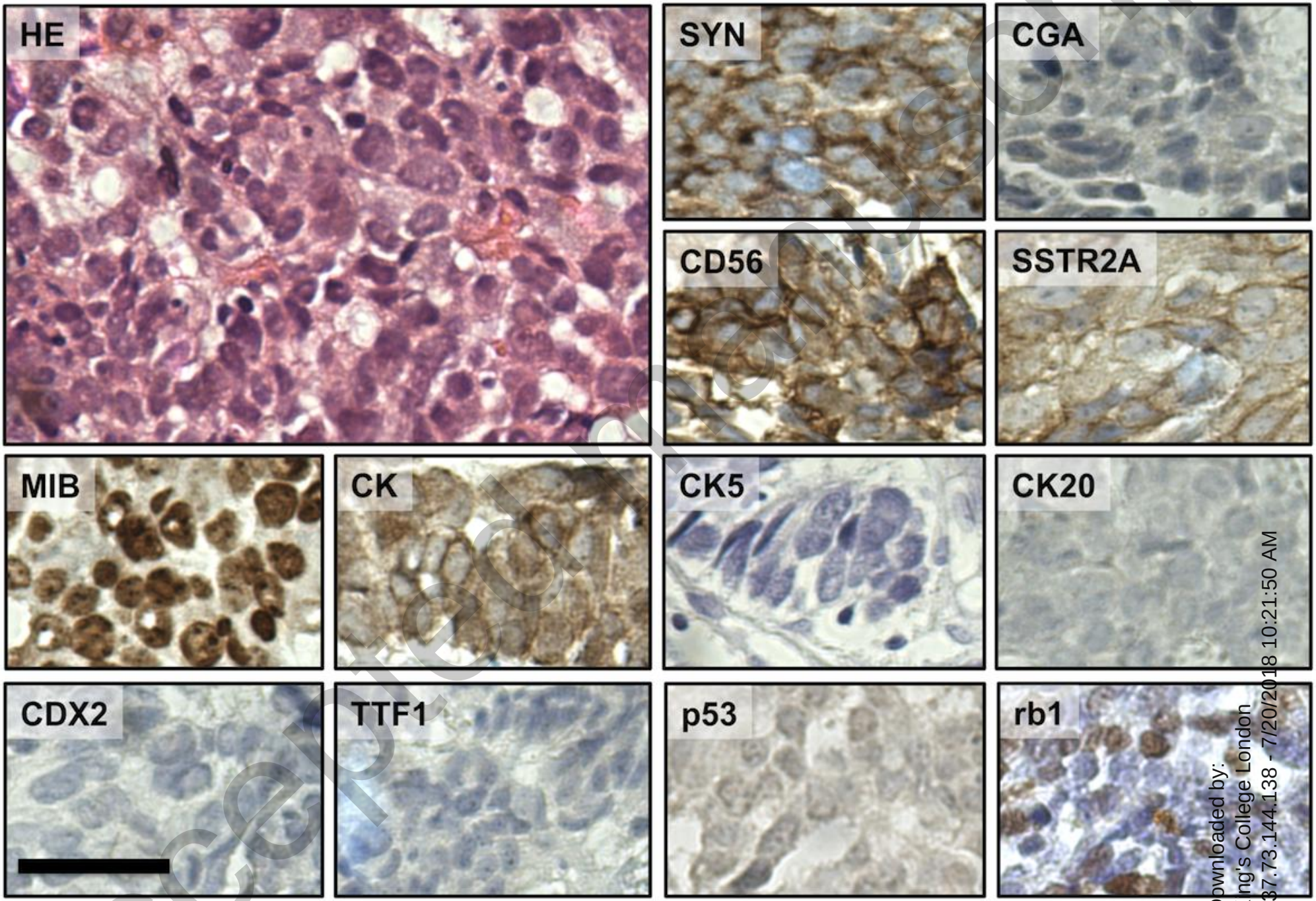

Figure 2.

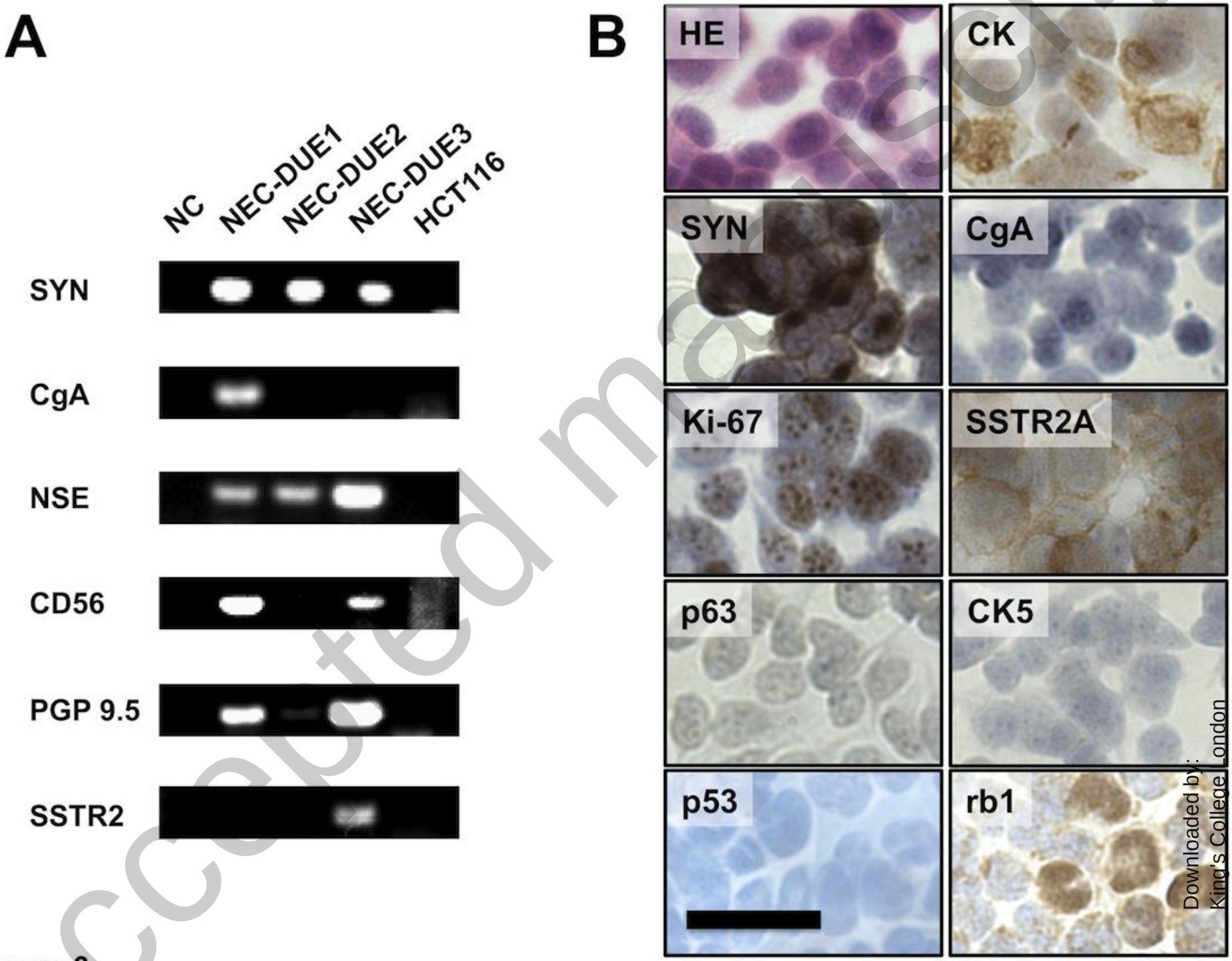

Figure 3.

Figure 4.

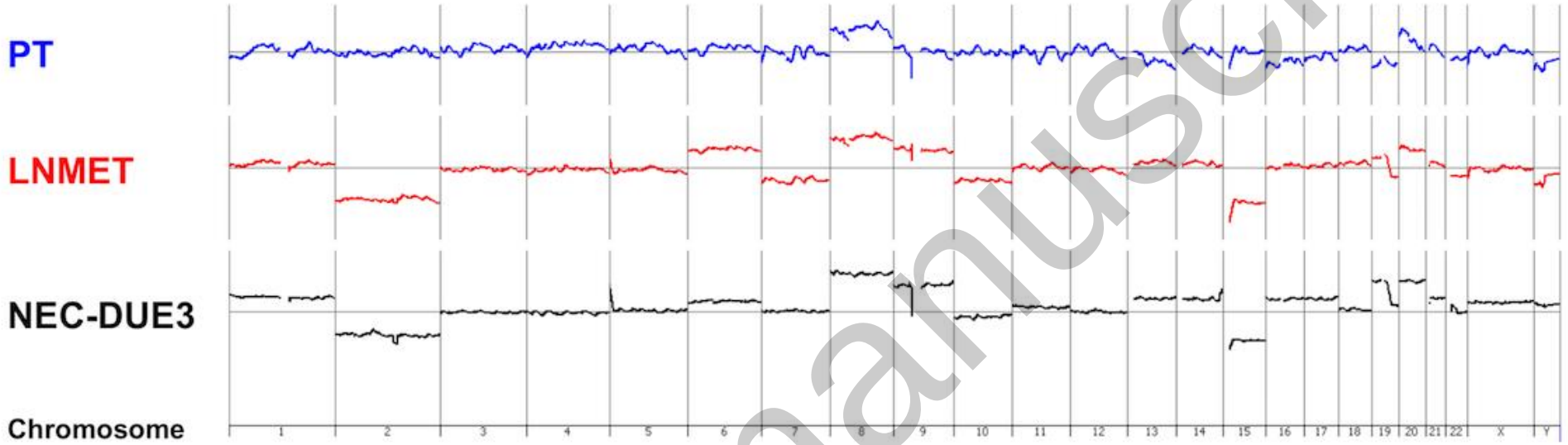

Figure 5.

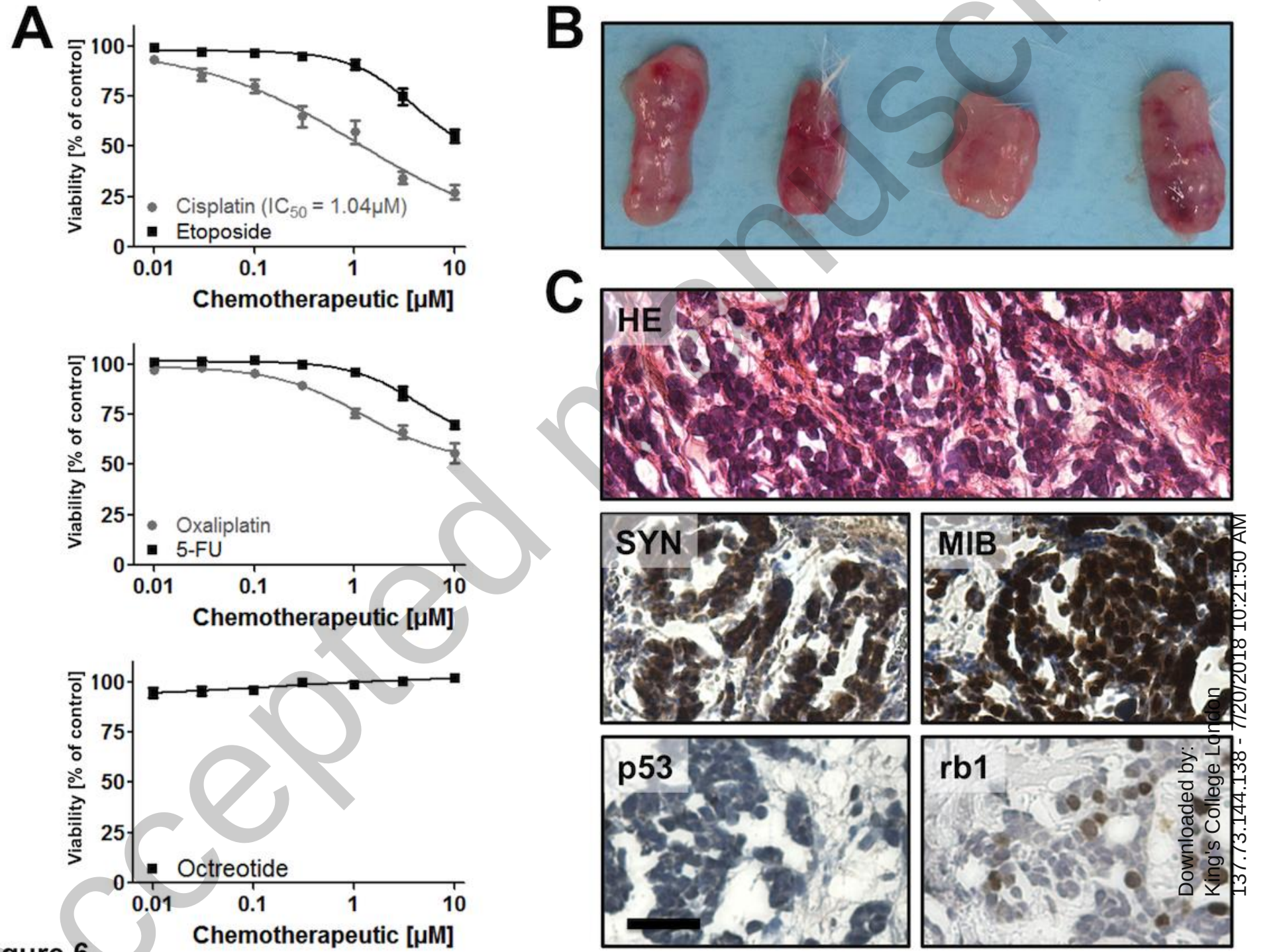

Figure 6.

Table 1: Antibodies used for immunohistochemistry and immunocytochemistry

Antigen	Code	Source	Dilution	Species
General neuroendocrine markers				
Synaptophysin	NCL-L-Synap 299	Novocastra, Berlin, Germany	1:100	Mouse, mAK
Chromogranin A	MAB 5268	Chemikon, Schwalbach, Germany	1:1000	Mouse, mAK
CD56/NCAM	IS628	Dako, Hamburg, Germany	1:50	Mouse, mAK
Somatostatin receptor				
SSTR 2A	SS-800	Gramsch Laboratories, Schwabhausen, Germany	1:10	Rabbit, pAK
Proliferation				
Ki-67	M7240	Dako, Hamburg, Germany	1:500	Mouse, mAK
Cytokeratins				
Pan-CK	MU071-UC	Biogenex, Fremont, CA, USA	1:250	Mouse, mAK
CK 5	XM26	Leica, Wetzlar, Germany	1:100	Mouse, mAK
CK 20	M7019	Dako, Hamburg, Germany	1:200	Mouse, mAK
Transcription factors				
TTF1	NCL-L-TTF	Novocastra, Berlin, Germany	1:200	Mouse, mAK
CDX2	MU392A-UC	Biogenex, Fremont, CA, USA	1:20	Mouse, mAK
p63	SFI-6	DCS, Hamburg, Germany	1:100	Mouse, mAK
p53	MABE327	Merck, Darmstadt, Germany	1:200	Mouse, mAK
Retinoblastoma Protein	554136	BD Pharmingen, Heidelberg, Germany	1:200	Mouse, mAK

Table 2: Primers used for RT-PCR

Primer	Gene name	5`-3`Sequence
SYN forward	Synaptophysin	cca atc aga tgt agt ctg gtc agt
SYN reverse		agg cct tct cct gag ctc tt
CGA forward	Chromogranin A	gcg gtt ttg aag atg aac tct c
CGA reverse		gct ctt cca ccg cct ctt
NSE forward	Neuron-specific enolase	act ttg tca ggg act atc ctg tg
NSE reverse		tcc cta cat tgg ctg tga act
CD56/NCAM forward	Neural cell adhesion molecule 1	tac cgc ggc aag aac atc
CD56/NCAM reverse		cca cct gca gag aaa ctg c
PGP9.5 forward	Protein gene product 9.5	cct gaa gac aga gca aaa tgc
PGP9.5 reverse		aaa tgg aaa ttc acc ttg tca tct
SSTR2 forward	Somatostatin receptor 2	gga gct agc gga ttg cag
SSTR2 reverse		cag cca gcc cag aga tct ta

Table 3. STR analysis of the primary tumor (PT), the lymph node metastasis (LNMET) and the cell line

STR Locus	PT	LNMET	Cell line
Amelogenin	XX	XX	XX
D3S1358	15-18	15-18	15-18
D1S1656	12-14	12-14	12-14
D6S1043	11-18	11-18	11-18
D13S317	11	11	11
Penta E	12	12	12
D16S539	11-12	11-12	11-12
D18S51	12-15	12-15	12-15
D2S1338	17-26	17	17
CSF1PO	11-12	11-12	11-12
Penta D	9	9	9
THO1	6	6	6
vWA	16-17	16-17	16-17
D21S11	27-29	27-29	27-29
D7S820	9-11	9-11	9-11
D5S818	11	11	11
TPOX	8-11	8-11	8
D8S1179	10-11	10-11	10-11
D12S391	18	18-19	18-19
D19S433	15-15.2	15-15.2	15-15.2
FGA	20-21	20-21	20-21